Investigation of inelastic electron tunneling spectra of metal-molecule-metal junctions fabricated using direct metal transfer method

Hyunhak Jeong,[1] Wang-Taek Hwang,[1] Pilkwang Kim,[1] Dongku Kim,[1] Yeonsik Jang,[1] Misook Min,[1] Dong Xiang,[2] Hyunwook Song,[3] Yun Daniel Park,[1] Heejun Jeong,[4,a)] and Takhee Lee[1,b)]

[1]*Department of Physics and Astronomy, Institute of Applied Physics, Seoul National University, Seoul 151-747, South Korea*
[2]*Institute of Modern Optics, Nankai University, Tianjin 300071, China*
[3]*Department of Applied Physics, Kyung Hee University, Yongin-si, Gyeonggi-do 446–701, South Korea*
[4]*Department of Applied Physics, Hanyang University, Ansan 426-791, South Korea*

(Received 5 December 2014; accepted 3 February 2015; published online 12 February 2015)

We measured the inelastic electron tunneling spectroscopy (IETS) characteristics of metal-molecule-metal junctions made with alkanethiolate self-assembled monolayers. The molecular junctions were fabricated using a direct metal transfer method, which we previously reported for high-yield metal-molecule-metal junctions. The measured IETS data could be assigned to molecular vibration modes that were determined by the chemical structure of the molecules. We also observed discrepancies and device-to-device variations in the IETS data that possibly originate from defects in the molecular junctions and insulating walls introduced during the fabrication process and from the junction structure. © *2015 AIP Publishing LLC*. [http://dx.doi.org/10.1063/1.4908185]

In the field of molecular electronics, extensive studies on the electrical properties of single molecules or self-assembled monolayers (SAMs) have been performed to understand the intrinsic charge transport mechanisms of molecular junctions and for realization of molecular-scale electronic devices.[1,2] Many researchers have reported numerous structures and platforms for fabricating molecular electronic junctions.[1,2] Among these, solid-state junction-based molecular electronic devices have the virtue of simple and massive production of molecular junctions for studying the charge transport characteristics using current-voltage characterization, temperature-variable analysis,[3] transition voltage spectroscopy,[4] and inelastic electron tunneling spectroscopy (IETS). In particular, IETS has been a powerful tool not only for verifying the existence of molecules in molecular junctions but also for investigating the effects of the molecules on the electronic charge transport characteristics.[5–9] Most of the IETS data were successfully obtained and analyzed from "pure" metal-molecule-metal junctions, where the molecules are simply bridged between two metal electrodes. Here, a pure metal-molecule-metal junction means a molecular junction fabricated without the involvement of any interlayers, such as conducting polymers or graphene films, in the junctions.[10] However, pure metal-molecule-metal junctions exhibit very low device yield because of the difficulty of forming a reliable electrical contact with the molecules because of electrical short problems.[11] To overcome this issue in a pure metal-molecule-metal junction structure, we reported a new approach for high-yield molecular junctions recently,[12] in which we performed various electrical characterizations, for example, current-voltage characterization and statistical analysis to confirm the molecular junctions. However, to strongly verify the formation of metal-molecule-metal junctions and the existence of molecules in the junctions, a more direct detection technique of molecules such as IETS is essential for this purpose. In addition, by investigating the IETS data, one can obtain information about the condition of molecular junctions such as the contact geometry and molecular conformation in the junctions.[5,13,14] Despite the importance, however, only a few studies have been reported, especially for SAM-based molecular junctions, mainly because of the difficulty of forming reliable junctions.[6,8,15,16] Therefore, it is necessary to perform the IETS experiments in a high-yield and reliable device testbed to accessibly investigate the intrinsic properties of the molecules.

In this study, we report on the IETS characteristics of alkanethiolate metal-molecule-metal junctions fabricated using a direct metal transfer (DMT) method, which we previously reported for high-yield metal-molecule-metal junctions without involving any interlayers. We could assign the measured IETS data to molecular vibration modes, which are clearly sensitive to the chemical structure of the molecules. With the observation, interestingly, we also observed discrepancies and device-to-device variations in the IETS data, such as negative values or dips, and peaks that cannot be assigned to any possible vibrational modes of the alkanethiolate molecules. We determined that these types of discrepancies and variations originate from the defects in the SAM, which result from the specific molecular device structure and device fabrication process.

Fig. 1(a) shows the process schematics for fabricating the molecular junctions. In this study, we used dodecanethiol ($HS(CH_2)_{11}CH_3$, denoted as C12) SAMs for the molecular junctions. The chemical structure of the molecule is presented in Fig. 1(b). To form the molecular junctions, we employed the DMT method that we previously reported.[12] Here, we briefly explain the fabrication procedure. First, conventional optical lithography was used to pattern the bottom Au (50 nm)/Ti (5 nm) electrodes on Si/SiO_2 substrates. Then,

a)Electronic mail: hjeong@hanyang.ac.kr
b)Electronic mail: tlee@snu.ac.kr

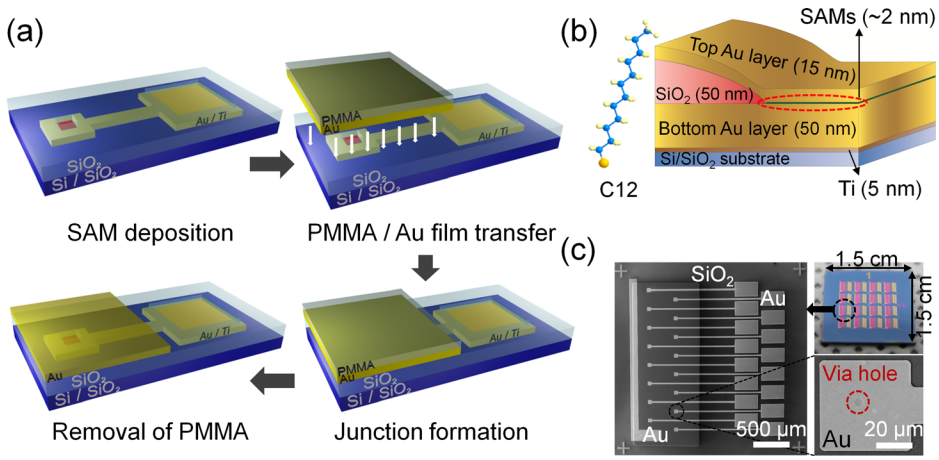

FIG. 1. (a) Schematics of molecular device fabrication procedure using DMT method. (b) Schematic illustration of the molecular junction with chemical structure of a dodecanethiol (C12) molecule. (c) SEM and optical microscopy images of the fabricated molecular devices.

the SiO_2 insulating walls (50 nm thick) were created using plasma-enhanced chemical vapor deposition. Circular holes (with radius of 2, 3, 4, and 5 μm) were made on the insulating wall to expose the Au bottom electrodes, and C12 SAMs were formed on the exposed Au surfaces by immersing the substrates in the SAM solution (~5 mM in anhydrous ethanol) in a N_2-filled glove box for 1–2 days (see upper left image of Fig. 1(a)). Then, a prepared poly(methyl methacrylate) (PMMA) film with patterned top electrode (15 nm-thick Au) was transferred on the substrate (upper right image of Fig. 1(a)), and the metal-molecule-metal junctions were formed (lower right image of Fig. 1(a)) by removing the remaining PMMA on the top electrode (lower left image of Fig. 1(a)). For detailed device fabrication procedures and conditions, refer to our previous report.[12] Fig. 1(b) presents a schematic illustration of the device junction structure, and Fig. 1(c) presents optical and scanning electron microscopy (SEM) images of fabricated molecular junctions using this DMT method. Using this method, we were able to considerably improve the device yield (~70%) as a pure metal-molecular-metal junction structure.[12]

The IETS measurements can be performed using various measurement circuit techniques.[18] Specifically, in our study, we adopted a standard AC modulation technique to investigate the IETS characteristics. Fig. 2(a) explains the schematic circuit diagram of our homemade IETS measurement system. The IETS measurement was performed at 4.2 K to reduce thermal broadening of the main signals with cryogenic measurement equipment.[5,6,8] The molecular devices were mounted on a 16-pin IC chip carrier socket on the sample stage inside a vacuum chamber that was electrically isolated from a power ground by a shield box before being dipped into a liquid-He-filled dewar. To measure the dI/dV and d^2I/dV^2 data directly, a standard AC lock-in technique was employed.[6,8] In practice, because only a small portion (<1%, as shown in Fig. S7(b) in the supplementary material[22]) of electrons exhibit inelastic tunneling behavior,[19] a high signal-to-noise measurement technique is essential to detect the IETS data. We used a 16-bit digital-to-analog converter (DAC), which was controlled by a laptop for DC bias voltages, and we used a reference signal of the lock-in amplifier (Stanford Research Systems 830) as an AC modulation bias. The DC bias voltages were swept from 0 to 0.4 V with an increment of 305 μV, and an AC modulation bias of 7.8 mV (RMS value) at a frequency of 1033 Hz was applied. After these two biases were added using a home-made voltage adder,[7,20] the bias was applied to the sample to obtain the second harmonic signals, proportional to d^2I/dV^2. Then, the output current signal was converted and amplified from a current signal to a voltage signal with a low-noise current amplifier (DL instrument 1211). Finally, using a phase-sensitive detector (PSD) in the lock-in amplifier and a digital multimeter (Agilent 34410A), the second harmonic signal, which is directly proportional to d^2I/dV^2, was measured.[7,8,20] Note that because of this PSD technique, the second harmonic signal has a higher signal-to-noise ratio than the numerical differentiation of the dI/dV data. To verify the inelastic tunneling process and our IETS measurement system, we performed IETS measurements on a resonant tunneling diode (RTD) device. An RTD is a diode with a resonant-tunneling structure, for which the I-V characteristics often exhibit negative differential resistance regions (NDRs).[21] This unique electrical characteristic enables an RTD to be a good test sample for examining our instrument setup. The lock-in 2ω measurement result, the numerical derivative of the lock-in 1ω measurement result, and the second numerical derivative of the I-V characteristics of an RTD test sample show similar trajectories with each other, which indicate that our measurement system is available to perform the IETS experiments (see Fig. S8 in the supplementary material[22]). In addition, another important finding here is that the numerical differentiation of the I-V characteristics exhibits 2ω spectra with a low signal-to-noise ratio, making it difficult to distinguish individual IETS peaks (see also Fig. S2 in the supplementary material[22]). Hence, a high signal-to-noise measurement technique such as the lock-in technique is essential to detect the IETS signal.

Fig. 2(b) shows the current density-voltage characteristics (J-V) of six selected C12 molecular junctions with pore sizes of 3 and 4 μm in radius that were used for IETS measurements in this study. Note that the molecular devices fabricated by the DMT method had already been characterized at room temperature (see Table S1 in the supplementary material[22] and Ref. 12); and in this present study, we performed the IETS experiments of a few molecular devices that were randomly selected based on a convenient location for chip-cutting and wire-bonding. These six C12 J-V data sets are presented as

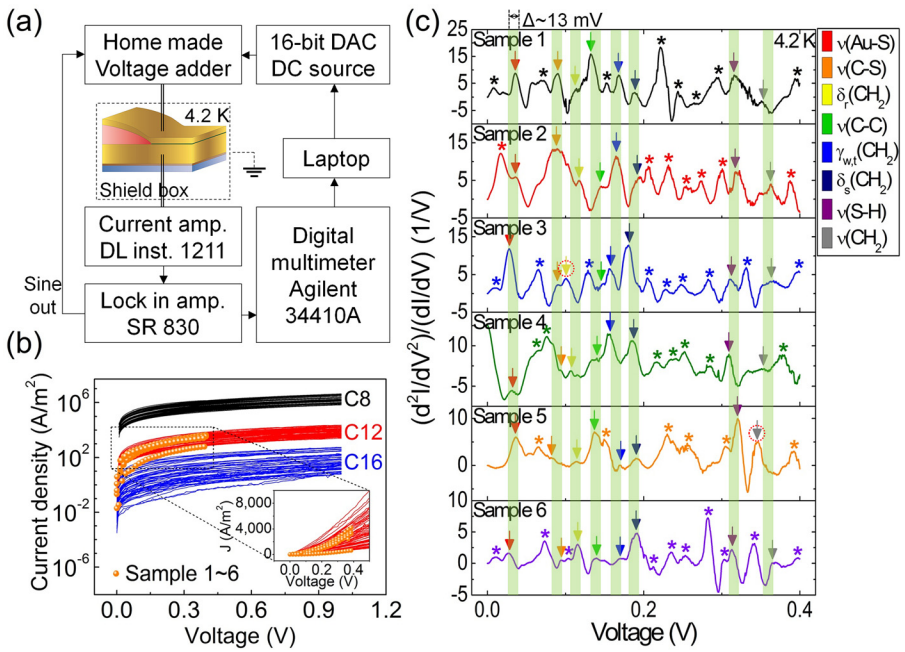

FIG. 2. (a) Circuit diagram of the IETS measurement system. (b) J-V characteristics of six different C12 molecular junctions (orange-colored circular symbols) with data sets of C8 and C16 molecular junctions. The inset shows J-V curves on the linear J scale. (c) IETS data of six C12 molecular junctions measured at 4.2 K. Each arrow indicates the corresponding molecular vibration modes of the C12 molecule. Peaks that cannot be assigned to any possible vibrational modes of the molecule are marked with asterisks. In this plot, shaded squares are used to compare each characteristic peak from device to device.

orange-colored circular symbols in distributions of J-V data sets (see Table S1 in the supplementary material[22]) for octanethiol ($HS(CH_2)_7CH_3$, denoted as C8), C12, and hexadecanethiol ($HS(CH_2)_{15}CH_3$, denoted as C16) for comparison (These were measured at room temperature).[12] Because alkanethiolates are insulating molecules with saturated alkyl chains, the overall transport mechanism is direct tunneling, which results in sigmoidal-shape curves in the individual I-V curves (inset of Fig. 2(b)) and exponential dependence of the current densities on the molecular length.[8,23] This dependency makes the tunneling current density (or conductance) decrease as the molecular length increases (i.e., conductance $\propto \exp(-\beta d)$, where β is the decay coefficient and d is the molecular length). As observed in Fig. 2(b), the current density of our working molecular junctions decreased as the number of carbon chains increased; we observed a β value of $\sim 1.0\,\text{Å}^{-1}$, which agrees with the literature values.[24] The selected six C12 samples exhibited consistent current density values upon bias sweep in the range of the C12 devices. It is noteworthy that the J-V characteristics of the molecular samples exhibit no particular features corresponding to vibrational modes of the molecules (see Fig. 2(b)); however, directly obtained dI/dV data (Fig. S1 in the supplementary material[22]) and d^2I/dV^2 data (Fig. 2(c)) proportional to the first and second harmonic signals from the lock-in amplifier exhibit distinctive trajectories, which can be assigned to the various vibrational modes of the C12 molecule.

Fig. 2(c) presents the IETS data measured at 4.2 K for the six C12 molecular junctions fabricated using the DMT method. Note that the I-V measurement results at room temperature using the probe station presented high device yields,[12] but the IETS measurements at 4.2 K requires several processes such as sample cutting, wire-bonding, chip mounting, and heat cycle to 4.2 K. So, by doing these steps, the initially working ultra-thin molecular junctions can easily become malfunctioning (mostly becoming electrical short) during the IETS experiments. Therefore, measuring many devices' IETS data is time-prohibitive. The spectra were stable upon successive bias sweep (see Fig. S3 in the supplementary material[22]), and the characteristic vibration peaks of the molecules were observed repetitively for different molecular junctions. We assigned the observed spectral peaks to specific molecular vibrations by comparison with previously reported infrared, Raman, high-resolution electron energy loss spectroscopy, IETS measurements, and density functional theory calculation results.[25–27] The peak positions related to molecular vibration of the six molecular junctions with its mean value and error (standard deviation) are summarized in Table I. The peaks are observed at approximately

TABLE I. Summary of vibrational modes assigned to the IETS spectra of Au-dodecanethiol-Au junctions.

Peak position (in mV)							
Sample 1	Sample 2	Sample 3	Sample 4	Sample 5	Sample 6	Mean value and error (standard deviation)	Mode assignment
35.4	35.1	28.1	31.7	35.4	27.8	32.3 ± 3.6	ν(Au-S)
89.1	88.5	89.1	93.4	85.1	94	89.9 ± 3.3	ν(C-S)
113.8	116.6	101.1	107.1	113.8	114.4	111.1 ± 5.9	$\delta_r(CH_2)$
133.9	144.6	146.5	138.6	137.3	139.2	140.0 ± 4.7	ν(C-C)
167.8	164.8	156.3	156.9	168.5	168.8	163.9 ± 5.8	$\gamma_{w,t}(CH_2)$
188.3	193.1	181	185.2	189.8	190.4	188.0 ± 4.3	$\delta_s(CH_2)$
317.1	318.9	311.9	310.7	319.8	312.8	315.2 ± 3.9	ν(S-H)
353.4	361.9	362.5	354.6	346.9	364.1	357.2 ± 6.7	$\nu(CH_2)$

30, 85, 105, 135, 160, 185, 315, and 360 mV, which correspond to ν(Au-S) stretching, ν(C-S) stretching, $\delta_r(CH_2)$ rocking, ν(C-C) stretching, $\gamma_{w,t}(CH_2)$ wagging, $\delta_s(CH_2)$ scissoring, ν(S-H) stretching, and $\nu(CH_2)$ stretching modes, respectively. Most of these peaks except $\delta_r(CH_2)$ of sample 3 and $\nu(CH_2)$ of sample 5 (marked as red circles in Fig. 2(c)) that represent the CH_2 rocking mode and CH_2 stretching mode were observed from all six molecular junctions in a certain range of the bias window (~13 mV), which indicates that the molecular junctions truly consisted of C12 molecules. In addition to these peaks, however, unexpected features in the IETS characteristics were also observed; some peaks could not be assigned to any possible molecular vibration modes (marked as asterisks in Fig. 2(c)) and dips.[8,15,28] In addition, the overall trajectories of each signal and normalized intensity of peaks ($(d^2I/dV^2)/(dI/dV)$) exhibited different behavior from device to device despite having similar J-V characteristics. The origin of these discrepancies in the IETS characteristics of molecular junctions will be discussed in detail later. Nonetheless, the overall accordance between the peak positions and referential vibration modes suggest that the IETS signal in Fig. 2(c) represents the vibrational characteristics of C12 molecular junctions. Also the spectra of opposite bias (negative bias) show almost anti-symmetric behaviors as expected (see Fig. S6 in the supplementary material[22]).

Now, let us analyze the discrepancies in the IETS characteristics. From theoretical studies of IETS characteristics in metal-molecule-metal junctions, negative values or dips in the IETS signal (d^2I/dV^2) are unexpected features because inelastic conduction channels related to molecular vibration modes remain open over a sufficient bias regime.[17] In well-controlled experimental studies, especially regarding single-molecule junctions, the correct IETS characteristics were observed.[7] However, in some cases, especially for SAM-based molecular junctions, an incorporation of defects, such as metal nanoparticles, into molecular junctions can introduce a hybrid metal particle-molecule electronic resonance state that can result in substantial modification of the intensity and line shape of the IETS signal such as negative values or dips.[29–31] In addition, the molecular conformations and contact geometry induced by the interaction between the electrode metal and molecular layer play an important role in the substantial modification of the IETS characteristics.[5,13,14] Theoretical investigations based on the resonance model also predicted that depending on the energetic parameters of the system, the contribution from the elastic component may be negative and, furthermore, may outweigh the positive contribution of the inelastic component, resulting in dips in the IETS characteristics.[30,32] This effect is a second-order effect in electron-vibration coupling, which may be related to reabsorption of molecular vibration by the elastic current component.[33]

Fig. 3 schematically illustrates the molecular junction structure that is formed by the DMT method in this study. Here, we draw the figure out of scale to emphasize the defects and irregular conformation of molecules. There can be several possible sources of defects as the electronic resonance states in the molecular junction. For example, the

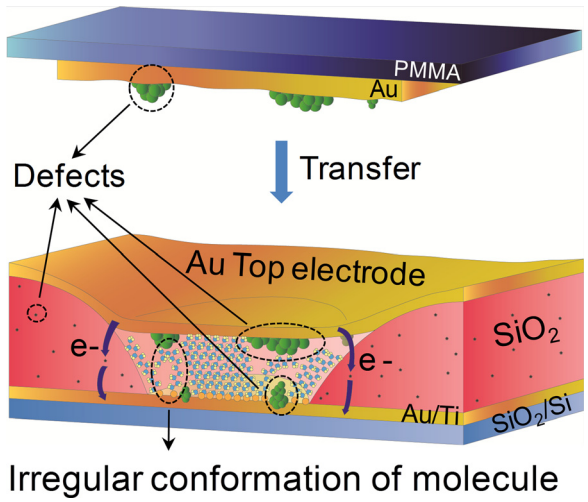

FIG. 3. Schematic illustration of a molecular junction structure formed by the DMT method.

defects can be formed in the SAMs because of small grains on the surface of the bottom contact (see Fig. S4 in the supplementary material[22]). Generally, these substrate-induced defects are proportional to the density of grain boundaries.[40] Also the top contact can induce defects in the SAMs. Due to the mechanical process, while preparing the top contact layer such as the detachment of the metal film from dummy substrates or cleaning of the film, the top contact surface has also small grains and mechanical defects (see Fig. S5 in the supplementary material[22]). These result in a poor contact with the SAMs, creating defects in the SAMs. The existence of these defects that results in poor contact properties with the SAMs can be indirectly revealed by estimating per-molecule conductance of our molecular junctions that would show relatively low conductance in comparison with the single molecule study cases assuming "perfect" array of single molecules (see the supplementary material[22]). Then, these types of additional resonance states can cause substantial modification to the intensity and line shape of the IETS characteristics such as negative values or dips.[29–31] With this unexpected feature, there are peaks that cannot be assigned to any possible vibrational modes of the C12 molecule (marked as asterisks in Fig. 2(c)). Because of the small size of the C12 molecule (~1.8 nm), the insulating SiO_2 layer cannot perfectly block the charge flow, especially at the edge of the layer, and thus, the defects in the insulating SiO_2 layer placed at the edge of the layer may also participate in the charge flow as hopping sites (Fig. 3). In this respect, these peaks are likely associated with the insulating SiO_2 layer or free thiol group.[16,20,34] According to previous studies, regarding the vibrational modes of silicon-based materials, several asterisks in Fig. 2(c) can be assigned to these vibrational modes.[34,35] With these background signals, the defect-induced resonance states may introduce virtual molecular vibrations, which also create the artificial peaks in the IETS signal.[31] Furthermore, in this study, the device-to-device variations in the IETS characteristics, for example, different peak intensity and line shape, were observed (Fig. 2(c)). These variations are related to the irregular conformations of molecules randomly caused by defects in the SAMs (Fig. 3),

which can be clearly identified by the log-normal variations in electrical characteristics.[12,14,36,37] Because the J-V characteristics of molecular junctions are an averaged effect of the charge flow through the entire SAM molecular junction, some randomly changed conformations of molecules in the molecular junction have less of an effect on the J-V characteristics, which eventually exhibit similar properties (Fig. 2(b)). The features of the IETS characteristics, such as peak positions or intensity, however, can be considerably modified by the individual change of conformations of molecules due to its highly sensitive nature on energy states between electrodes.[30,31] In addition, the irregular conformations of molecules change the scattering cross-sections of the molecular vibration modes along the transport pathway, which results in modification in the strength of electron-molecular vibration coupling and eventually the peak intensity.[18,38] Indeed, the modifications of IETS spectra by different molecular conformations have been observed even in the single molecule junction.[5] Therefore, defect-induced arbitrary changes of molecular conformations in the SAM of each molecular junction result in device-to-device variations of the IETS characteristics. Although these analyses are fairly reasonable, we think that there should be more delicate investigations on the analysis of IETS characteristics in future.

Nonetheless, the overall accordance between peak positions and the referential vibration modes and its repeatability and similarity with the numerical derivative of the first harmonic signal (Figs. S2 and S3 in the supplementary material[22]) demonstrate that the IETS signals obtained in this study represent molecular vibrational characteristics of C12 molecules along with other artificial features. It is suggested that one should fabricate defect-free and even molecular junctions without the insulating layer at the edge of the junction to obtain an accurate IETS signal and avoid the discrepancies. In another sense, it is helpful to eliminate the device-to-device variations of the IETS characteristics by statistically collecting the IETS peak positions from a sufficiently large number of molecular junctions.[39]

In summary, we have demonstrated the measurements of molecular vibration spectra for alkanethiolate metal-molecule-metal junctions prepared by the direct metal transfer method using the IETS technique. We observed that the measured IETS signal can be assigned to molecular vibration modes that are sensitive to the chemical structure of the molecules. In addition, we were able to analyze possible defects in the molecular junctions which were not revealed by the current-voltage characteristics or temperature-variable analysis. The defects appeared as discrepancies and device-to-device variations in the IETS characteristics, which originated from the additional electronic resonant states and the irregular conformations of molecules induced by metal defects placed in the molecular junctions or the insulating SiO_2 layer.

The authors appreciate the financial support received from the National Creative Research Laboratory program (Grant No. 2012026372) and from the National Core Research Center program (Grant No. R15-2008-006-03002-0) through the National Research Foundation of Korea (NRF). Y.D.P. acknowledges the financial support received from the NRF (2014-023563), and H.S. acknowledges the support by Basic Science Research Program (NRF-2013R1A1A1076158).

[1]J. C. Love, L. A. Estroff, J. K. Kriebel, R. G. Nuzzo, and G. M. Whitesides, Chem. Rev. **105**, 1103 (2005).
[2]H. Song, M. A. Reed, and T. Lee, Adv. Mater. **23**, 1583 (2011).
[3]S. H. Choi, B. Kim, and C. D. Frisbie, Science **320**, 1482 (2008).
[4]J. M. Beebe, B. Kim, J. W. Gadzuk, C. D. Frisbie, and J. G. Kushmerick, Phys. Rev. Lett. **97**, 026801 (2006).
[5]Y. Kim, H. Song, F. Strigl, H.-F. Pernau, T. Lee, and E. Scheer, Phys. Rev. Lett. **106**, 196804 (2011).
[6]J. G. Kushmerick, J. Lazorcik, C. H. Patterson, R. Shashidhar, D. S. Seferos, and G. C. Bazan, Nano Lett. **4**, 639 (2004).
[7]H. Song, Y. Kim, Y. H. Jang, H. Jeong, M. A. Reed, and T. Lee, Nature **462**, 1039 (2009).
[8]W. Y. Wang, T. Lee, I. Kretzschmar, and M. A. Reed, Nano Lett. **4**, 643 (2004).
[9]L. H. Yu, Z. K. Keane, J. W. Ciszek, L. Cheng, M. P. Stewart, J. M. Tour, and D. Natelson, Phys. Rev. Lett. **93**, 266802 (2004).
[10]G. Wang, T.-W. Kim, and T. Lee, J. Mater. Chem. **21**, 18117 (2011).
[11]B. de Boer, M. M. Frank, Y. J. Chabal, W. R. Jiang, E. Garfunkel, and Z. Bao, Langmuir **20**, 1539 (2004).
[12]H. Jeong, D. Kim, P. Kim, M. R. Cho, W.-T. Hwang, Y. Jang, K. Cho, M. Min, D. Xiang, Y. D. Park, H. Jeong, and T. Lee, Nanotechnology **26**, 025601 (2015).
[13]L.-L. Lin, C.-K. Wang, and Y. Luo, ACS Nano **5**, 2257 (2011).
[14]A. Troisi and M. A. Ratner, Phys. Chem. Chem. Phys. **9**, 2421 (2007).
[15]W. Wang and C. A. Richter, Appl. Phys. Lett. **89**, 153105 (2006).
[16]W. Wang, A. Scott, N. Gergel-Hackett, C. A. Hacker, D. B. Janes, and C. A. Richter, Nano Lett. **8**, 478 (2008).
[17]J. Lambe and R. C. Jaklevic, Phys. Rev. **165**, 821 (1968).
[18]L. Lin, J. Jiang, and Y. Luo, Physica E **47**, 167 (2013).
[19]B. N. J. Persson, Phys. Scr. **38**, 282 (1988).
[20]H. Song, Y. Kim, J. Ku, Y. H. Jang, H. Jeong, and T. Lee, Appl. Phys. Lett. **94**, 103110 (2009).
[21]R. Tsu and L. Esaki, Appl. Phys. Lett. **22**, 562 (1973).
[22]See supplementary material at http://dx.doi.org/10.1063/1.4908185 for the measurement results of the first harmonic signal (dI/dV) of a C12 molecular junction, comparison between the lock-in 2ω data and the numerical derivative, the IETS data of a C12 molecular junction under repeated measurements, summary of device statistics, surface morphological image of both top and bottom electrodes, estimation of conductance per a single molecule, IETS data of a sample both at negative and positive bias regimes, principle of IETS and I-V, dI/dV, and d^2I/dV^2 characteristics of a RTD sample.
[23]T.-W. Kim, G. Wang, H. Lee, and T. Lee, Nanotechnology **18**, 315204 (2007).
[24]H. Song, C. Lee, Y. Kang, and T. Lee, Colloids Surf., A **284**, 583 (2006).
[25]M. A. Bryant and J. E. Pemberton, J. Am. Chem. Soc. **113**, 8284 (1991).
[26]C. Castiglioni, M. Gussoni, and G. Zerbi, J. Chem. Phys. **95**, 7144 (1991).
[27]H. S. Kato, J. Noh, M. Hara, and M. Kawai, J. Phys. Chem. B **106**, 9655 (2002).
[28]M. Taniguchi, M. Tsutsui, K. Yokota, and T. Kawai, Nanotechnology **20**, 434008 (2009).
[29]A. Bayman, P. K. Hansma, and W. C. Kaska, Phys. Rev. B **24**, 2449 (1981).
[30]M. Galperin, M. A. Ratner, and A. Nitzan, J. Chem. Phys. **121**, 11965 (2004).
[31]L. H. Yu, C. D. Zangmeister, and J. G. Kushmerick, Phys. Rev. Lett. **98**, 206803 (2007).
[32]T. Mii, S. G. Tikhodeev, and H. Ueba, Phys. Rev. B **68**, 205406 (2003).
[33]B. N. J. Persson and A. Baratoff, Phys. Rev. Lett. **59**, 339 (1987).
[34]K. K. Irikura, J. Phys. Chem. Ref. Data **36**, 389 (2007).
[35]C. Petit, G. Salace, and D. Vuillaume, J. Appl. Phys. **96**, 5042 (2004).
[36]Q. Fu, Y. Luo, J. Yang, and J. Hou, Phys. Chem. Chem. Phys. **12**, 12012 (2010).
[37]L. Vitali, S. D. Borisova, G. G. Rusina, E. V. Chulkov, and K. Kern, Phys. Rev. B **81**, 153409 (2010).
[38]J. Hihath and N. Tao, Prog. Surf. Sci. **87**, 189 (2012).
[39]J. Fock, J. K. Sorensen, E. Loertscher, T. Vosch, C. A. Martin, H. Riel, K. Kilsa, T. Bjornholm, and H. van der Zant, Phys. Chem. Chem. Phys. **13**, 14325 (2011).
[40]E. A. Weiss, R. C. Chiechi, G. K. Kaufman, J. K. Kriebel, Z. Li, M. Duati, M. A. Rampi, and G. M. Whitesides, J. Am. Chem. Soc. **129**, 4336 (2007).